Measurement of the perpendicular rotation-tunneling spectrum of the water dimer by tunable far infrared laser spectroscopy in a planar supersonic jet

Kerry L. Busarow, R. C. Cohen, Geoffrey A. Blake,[a] K. B. Laughlin,[b] Y. T. Lee, and R. J. Saykally

Department of Chemistry and Materials and Chemical Sciences Division, University of California and Lawrence Berkeley Laboratories, Berkeley, California 94720

(Received 31 October 1988; accepted 19 December 1988)

Fifty-six transitions from the $K = 1$ lower $\rightarrow K = 2$ lower tunneling–rotation band of water dimer have been measured and assigned at 22 cm^{-1} by direct absorption spectroscopy in a cw planar supersonic jet expansion using a tunable far infrared laser spectrometer. Two different models were used to fit the data and several spectroscopic constants were determined for the upper and lower states. This work supports the local IAM model recently proposed by Coudert and Hougen for the hydrogen bond tunneling dynamics of the water dimer. This model includes four different tunneling motions, all of which contribute to the observed tunneling splittings. This is the most complicated hydrogen bonded system considered to be well understood at this time, at least in the lowest few K states.

INTRODUCTION

The water dimer is of considerable significance in chemistry and biology as a prototype for understanding local structure and hydrogen bond dynamics in condensed phases. The molecular beam electric resonance (MBER) studies of Dyke and co-workers[1–5] have provided an important initial basis for establishing a quantitative undertanding of this very complex system. In particular, the molecular structure of $(H_2O)_2$ deduced from the MBER experiments has confirmed *ab initio* predictions of a tetrahedrally bonded "*trans*-linear" ground state[6] (Fig. 1) and these results clearly evidenced the complicated nature of hydrogen exchange tunneling motions. However, progess in obtaining a more complete understanding of this important phenomenon has been severely impeded by the lack of an appropriate theoretical model for such multidimensional tunneling processes. The recent work of Coudert and Hougen[7] promises important new advances in this endeavor.

Very recently, Fourier transform microwave spectroscopy of $(H_2O)_2$ carried out by Coudert *et al.*[8] and measurements of the OH stretching vibration–rotation spectrum by Huang and Miller[9] have yielded a considerable amount of new data, supplemented by additional MBER measurements from the Dyke group.[10] Altogether, these high resolution spectroscopy experiments have produced precise measurements of over 90 rotation–tunneling transitions, and it would seem that such a large amount of data would be sufficient to characterize most of the relevant tunneling dynamics, given an appropriate theoretical formalism. In fact, this is not the case. The microwave and MBER transitions are all a-type ($\Delta K = 0$) and are restricted to sampling only one of the two principal tunneling motions, viz., the low frequency donor–acceptor tunneling. As a result, both the A rotational constant and the much larger acceptor tunneling splittings remain to be determined, and these properties are clearly essential for developing a meaningful model for the hydrogen tunneling dynamics.

In this paper we report the measurement of perpendicular ($\Delta K = +1$) rotation–tunneling transitions of $(H_2O)_2$ by a new technique developed recently at Berkeley—tunable far infrared laser spectroscopy of planar supersonic jets. Over 350 transitions have been measured in an argon–water supersonic jet expansion in the range from 510 to 835 GHz. Of these, 56 have been assigned to a rotation–tunneling band originating in the lower acceptor tunneling level of $K = 1$ and terminating at the lower acceptor tunneling level of $K = 2$. Over 85 of the remaining lines have been assigned to ArH_2O,[11] and 200 remain unassigned.

EXPERIMENTAL

The experimental apparatus has been described in detail elsewhere.[12,13] In the present experiments, conditions were identical to those in the ArH_2O study.[11] The water dimers are formed in a cw planar supersonic expansion. The nozzle is 1.5 in. long and 0.002 in. wide and is operated without temperature control. Argon is blown over water at room temperature to produce the gas mixture. Previously, the ar-

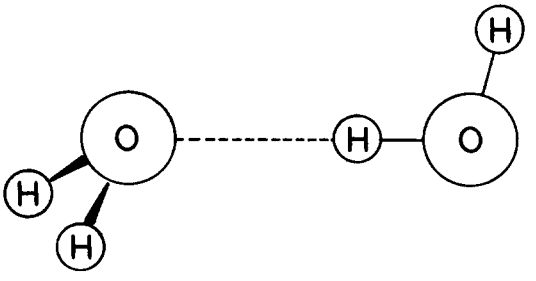

FIG. 1. The *trans*-linear structure of the water dimer.

[a] Berkeley Miller Postdoctoral Fellow; present address: Center for Cosmochemistry and Geochemistry, Division of Geology and Planetary Sciences, California Institute of Technology, Pasadena, CA 91125.

[b] Present address: Department of Chemistry, Massachusetts Institute of Technology, Cambridge, MA 02139.

 0021-9606/89/083937-07$02.10 © 1989 American Institute of Physics

Downloaded 08 Mar 2006 to 131.215.225.174. Redistribution subject to AIP license or copyright, see http://jcp.aip.org/jcp/copyright.jsp

gon was bubbled through the water, however, this resulted in a prohibitive amount of water being bumped into the gas manifold and signals were not consistent in time. The water was obtained from the distilled water tap and the Ar is 99.99% pure (liquid air). The expansion was typically operated with between 800 and 1000 Torr behind the nozzle and approximately 100 mTorr in the vacuum chamber, which is pumped by a 2650 cfm Roots blower. Far infrared radiation is produced with a cw tunable far infrared laser system similar to that of Pickett and co-workers.[14] Production of coherent FIR radiation occurs through nonlinear mixing of fixed frequency FIR radiation with tunable microwave radiation in a GaAs Schottky barrier diode. Linewidths observed are approximately 400 kHz (FWHM), resulting from residual Doppler broadening in the planar jet.

The precision of the frequency measurement is approximately 1 MHz, resulting from the necessity of shifting the fixed frequency FIR laser slightly to determine which sideband is responsible for a given absorption. The FIR laser is then reset to the maximum of the gain curve. This is a rather imprecise procedure. When we carefully calibrate each line with a known reference, we can obtain uncertainties of less than 50 kHz,[13] however, this is a painstaking process for a large number of lines, and it is seldom that the available models require that high a level of precision.

The typical signal to noise ratio in the water dimer spectra is less than 50, with a time constant of 300 ms. For other van der Waals clusters, such as ArH_2O, ArHCl, and $(HCl)_2$, under similar conditions, S/N of $\geqslant 1000$ was achieved. This indicates that the perpendicular dipole moment of water dimer is quite small, assuming that we are producing a similar density of dimers, in agreement with the MBER results of Dyke and co-workers.[4]

ANALYSIS

The rotation–tunneling energy level diagram for the water dimer is explained in the papers of Coudert *et al.*[8] and by Odutola *et al.*[10] and will only be discussed here as is necessary to describe the assignment of the far infrared spectra. The equilibrium structure of water dimer is the *trans*-linear form, determined from the experimental work of Dyke and co-workers,[4] in agreement with theoretical predictions[6] (Fig. 1). It contains a single nearly linear hydrogen bond, with a strength of approximately 5 kcal/mol, and has a plane of symmetry (C_s). The A rotational constant is estimated to be approximately 6 cm^{-1}, and B and C are ~ 6 GHz (0.2 cm^{-1}).

There are several different types of feasible proton tunneling motions considered in this model. The first, which Coudert *et al.* refer to as a $1 \rightarrow 4$ tunneling,[8] involves the exchange of the two hydrogens on the acceptor molecule. We will refer to this as the *acceptor* tunneling. The numbers 1 and 4 refer to tunneling between the frameworks 1 and 4 of the eight possible frameworks for water dimer as labeled by Coudert *et al.*[8] (Fig. 2). No hydrogen bond is broken in this exchange. The second tunneling motion, referred to by Coudert *et al.* as a $1 \rightarrow 5,6$ tunneling, or a geared internal rotation, exchanges the donor proton involved in the hydrogen bond with a proton from the acceptor molecule. Hence, we refer to

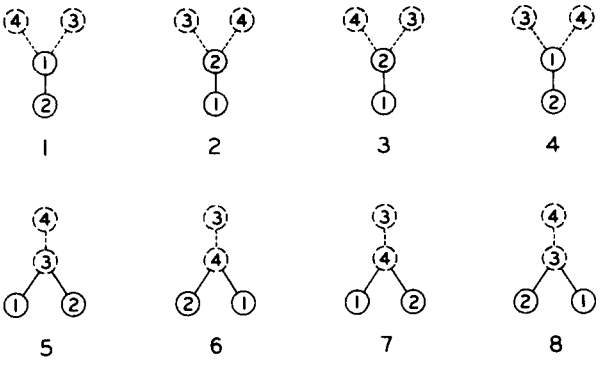

FIG. 2. The eight equivalent frameworks for the water dimer from Coudert *et al.* (Ref. 8) are used to label the various tunneling motions between frameworks. In this representation, the oxygen atoms are not shown, only the hydrogens, labeled 1 through 4. The dashed lines indicate the hydrogens are behind the plane of the figure and solid lines indicate the hydrogens are above the plane.

this as the *geared donor–acceptor* tunneling. In this tunneling motion, the roles as hydrogen acceptor and donor are reversed. This motion does involve breaking and reforming the hydrogen bond and is analogous to the trans geared motion in $(HF)_2$.[15] The donor–acceptor tunneling leads to a splitting of each rotational state into four levels, two of which are degenerate, thereby resulting in three actual levels for each value of J (for $K = 0$). The overall tunneling splitting associated with this motion is 19 GHz for $K = 0$.[10] The acceptor tunneling motion causes an additional doublet splitting of all these levels. Because this motion does not involve any bond breakage, it is expected to result in a considerably larger tunneling splitting than the geared donor–acceptor tunneling; Coudert *et al.*[8] have estimated it to be 6 cm^{-1} for $K = 0$. Therefore, for each J in $K = 0$, there are six levels, two of which are doubly degenerate (the E states). An additional possible tunneling motion is the $1 \rightarrow 2$ tunneling, also called a geared inversion. Although the $1 \rightarrow 4$ and the $1 \rightarrow 5$ tunneling motions split the levels into the maximum number of levels allowed by the group theory (into six states for each J), the $1 \rightarrow 2$ tunneling can cause an additional shift in the energy of these states. Coudert and Hougen[7] have proposed that for K even states, the A/B states would be shifted upward relative to the energies from the other two tunneling splittings, and the E states would be pushed down, where for K odd, the levels would shift in the opposite direction. The extent of the perturbation due to the $1 \rightarrow 2$ tunneling on the energy of the states is yet to be determined. One final tunneling motion considered by Coudert and Hougen is the $1 \rightarrow 7$ or the antigeared donor–acceptor tunneling, analogous to an antigeared motion in $(HF)_2$. This tunneling would also cause a shift in the energies and would result in slightly different selection rules. For the present discussion, we will ignore the $1 \rightarrow 7$ tunneling and assume that the $1 \rightarrow 2$ tunneling need not be explicitly considered because it will result in a systematic shift of all the lines that we measure. Although the E state transitions would be shifted in the opposite direction, we have not observed these transitions due to their low population in the jet, as will be discussed below. The $1 \rightarrow 2$ tunneling, however, most likely plays a significant

Downloaded 08 Mar 2006 to 131.215.225.174. Redistribution subject to AIP license or copyright, see http://jcp.aip.org/jcp/copyright.jsp

role in the observed transition frequencies. Therefore, for $K = 0$ there exist six levels. For each value of J, the lower set of three levels, which we will henceforth refer to as "$K = 0$ lower," and the upper set of three levels, "$K = 0$ upper," are separated by the acceptor tunneling splitting ($\sim 6\ \mathrm{cm}^{-1}$). For $K \neq 0$, there is an additional splitting caused by the asymmetry doubling. This asymmetry splitting is significantly smaller than the other two tunneling splittings, such that for $K \neq 0$, there will be twelve levels for each value of J, six lower levels and six upper levels. An energy level diagram is shown in Fig. 3, including the two lowest rotational states for each value of K. The asymmetry splitting is not shown on this diagram because it is too small to be visible on this scale.

In the present work, we have measured transitions from the $K = 1$ lower states to the $K = 2$ lower states (Fig. 3). Coudert *et al.*[8] point out that they had made an arbitrary choice between two different possible schemes for labeling the state symmetries in $K \neq 0$, due to the ambiguity in the sign of the asymmetry splitting. The experimental results then available could not establish which of these was correct. The recent work of Huang and Miller[9] demonstrated that their choice was incorrect, based on the relative intensities of the observed lines (the statistical weights for the $A_2^{\pm}$ and $B_2^{\pm}$ states are three and six, respectively). Our work confirms this conclusion. In Fig. 4 we present spectra for two transitions originally labeled $Q(3)A_2^{+}$ and $Q(3)B_2^{-}$ by Coudert *et al.* However, the 2:1 intensity ratio clearly indicates that these labels should be switched, in agreement with Huang and Miller. It is difficult to measure intensity ratios over a large frequency range on this spectrometer due to laser power fluctuations. However, the fluctuation in laser power decreases for closely spaced transitions and in the case of Q branch transitions, we believe that these intensity measurements are quite reliable.

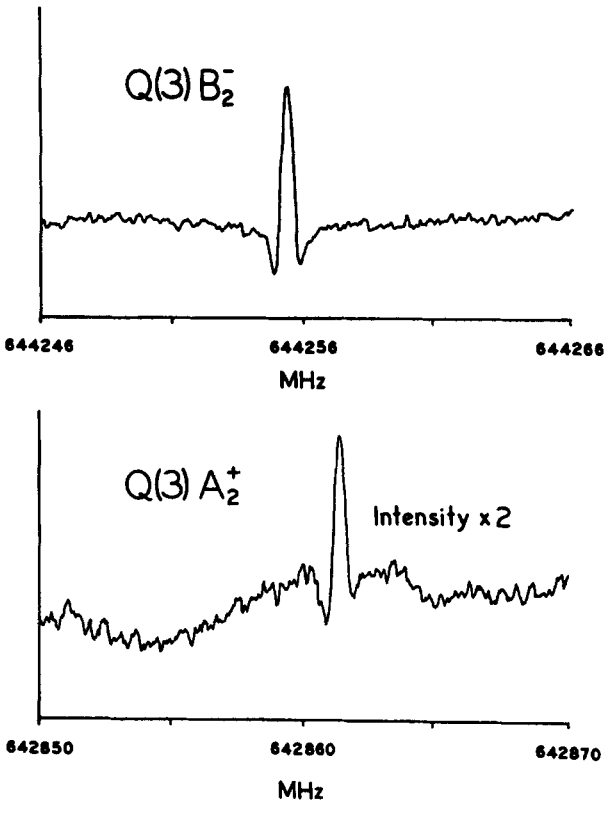

FIG. 4. A comparison of the intensities for two of the $Q(3)$ transitions. The upper scan is B_2^- symmetry, spin weight equal to six, and the lower scan is A_2^+ symmetry, spin weight equal to three. The lower scan intensity is multiplied by a factor of 2.

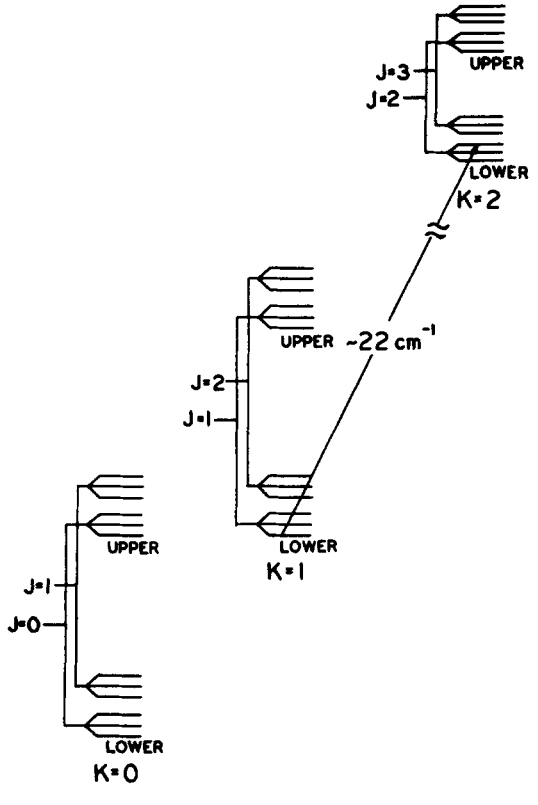

FIG. 3. The energy level diagram for the water dimer including the two lowest rotational states for each K. The asymmetry splittings for $K = 1$ and 2 are not shown. The splitting between the states labeled "lower" and "upper" is the result of the $1 \rightarrow 4$ (acceptor) tunneling. The smaller triplet splitting is the result of the $1 \rightarrow 5$ (greared donor–acceptor) tunneling.

Given the triplet level structure of each J state resulting from the donor–acceptor tunneling splitting (ignoring the asymmetry splitting), one expects to observe three bands slightly shifted from one another, each exhibiting P, Q, and R branches. In our spectra, however, only two bands are observed, with Q branches at 644 and 670 GHz. We find no transitions originating from the $E^{\pm}$ states. This results from the fact that in the cold jet expansion, the population in the $E^{\pm}$ states can relax to the $K = 0$ lower $E^{\pm}$ states. The other states, of $A_2^{\pm}$ and $B_2^{\pm}$ symmetry, can only relax to the $K = 0$ upper state because of the selection rules, $A_2 \leftrightarrow A_2$ and $B_2 \leftrightarrow B_2$. Coudert and co-workers[8] were the first to assign transitions originating in $K = 1$ lower in a cold jet, and because they observed transitions in $K = 0$ upper as well, they proposed that the $K = 0$ upper and $K = 1$ lower levels must be nearly degenerate for there to be significant population in both states in the 1 K supersonic expansion. Based on this assumption, they proposed that the $K = 0$ lower to $K = 0$ upper splitting (the acceptor tunneling splitting) was 6 cm^{-1}, assuming that $A = 6\ \mathrm{cm}^{-1}$. As in the present spectra, Coudert and co-workers only observed $A_2^{\pm}/B_2^{\pm}$ transitions

Downloaded 08 Mar 2006 to 131.215.225.174. Redistribution subject to AIP license or copyright, see http://jcp.aip.org/jcp/copyright.jsp

TABLE I. Frequencies for transitions from $K = 1$ lower to $K = 2$ lower in $(H_2O)_2$. Calculated frequencies are determined from the constants of the first two fits shown in Table II. Transitions are labeled by the symmetry and rotational level of the initial state. The lower band originates in the lower pairs of K-type doublets of $K = 1$ lower and terminates in the upper pairs of K-type doublets of $K = 2$ lower. The upper band originates in the upper pairs of K-type doublets of $K = 1$ lower and terminates in the lower pairs of K-type doublets in $K = 2$ lower. The last four transitions in each band are calculated from observed microwave transitions of Coudert *et al.* (Ref. 8). All frequencies are in MHz.

	Lower band $K = 1$ lower $\rightarrow K = 2$ lower		
Transition	Observed frequency	Calculated frequency	Obs.-calc.
$P(5)B_2^+$	607 247.3	607 240.0	7.3
$P(5)A_2^-$	610 301.8	610 305.1	− 3.3
$P(4)B_2^+$	622 426.4	622 427.6	− 1.2
$P(3)B_2^+$	633 305.1	633 310.8	− 5.7
$P(3)A_2^-$	634 590.0	634 589.0	1.0
$Q(7)B_2^+$	666 904.4	666 913.6	− 9.2
$Q(6)A_2^-$	667 883.5	667 873.6	9.9
$Q(6)B_2^+$	672 042.4	672 043.2	− 0.8
$Q(5)B_2^+$	668 777.2	668 769.1	8.1
$Q(5)A_2^-$	671 832.6	671 834.3	− 1.7
$Q(4)A_2^-$	669 565.3	669 566.6	− 1.3
$Q(4)B_2^+$	671 659.4	671 658.4	1.0
$Q(3)B_2^+$	670 232.4	670 238.3	− 5.9
$Q(3)A_2^-$	671 519.8	671 516.5	3.3
$Q(2)A_2^-$	670 757.1	670 761.6	− 4.5
$Q(2)B_2^+$	671 414.8	671 409.4	5.4
$R(1)B_2^+$	695 741.2	695 740.3	0.9
$R(1)A_2^-$	695 963.1	695 958.1	5.0
$R(2)A_2^-$	707 684.0	707 689.1	− 5.1
$R(2)B_2^+$	708 339.2	708 336.9	2.3
$R(3)B_2^+$	719 463.0	719 469.1	− 6.1
$R(3)A_2^-$	720 749.1	720 747.3	1.8
$R(4)A_2^-$	731 095.0	731 095.8	− 0.8
$R(4)B_2^+$	733 185.6	733 187.5	− 1.9
$R(5)B_2^+$	742 598.5	742 590.3	8.2
$R(5)A_2^-$	745 652.1	745 655.5	− 3.4
$R(6)B_2^+$	758 144.0	758 149.0	− 5.0
$R(7)B_2^+$	765 293.9	765 295.3	− 1.4
$R(8)B_2^+$	783 204.9	783 201.8	3.1
$K = 1$ lower			
$J = 1B_2^+ \rightarrow J = 2B_2^+$	24 327.462	24 330.8	− 3.3
$J = 1A_2^- \rightarrow J = 2A_2^-$	25 206.003	25 196.5	9.5
$J = 2A_2^- \rightarrow J = 3A_2^-$	36 164.855	36 172.6	− 7.7
$J = 2B_2^+ \rightarrow J = 3B_2^+$	38 108.343	38 098.6	9.7
	Upper band $K = 1$ lower $\rightarrow K = 2$ lower		
Transition	Observed frequency	Calculated frequency	Obs.-calc.
$P(4)B_2^-$	592 927.3	592 934.0	− 6.7
$P(3)B_2^-$	607 318.0	607 315.6	2.4
$Q(8)B_2^-$	638 504.6	638 535.6	− 31.0
$Q(7)A_2^+$	639 522.6	639 491.4	31.1
$Q(6)B_2^-$	640 478.9	640 447.9	31.0
$Q(5)A_2^+$	641 367.0	641 357.2	9.8
$Q(5)B_2^-$	644 611.4	644 610.9	0.5
$Q(4)B_2^-$	642 167.6	642 178.1	− 10.5
$Q(4)A_2^+$	644 412.4	644 415.1	− 2.7
$Q(3)A_2^+$	642 859.2	642 876.2	− 17.0
$Q(3)B_2^-$	644 253.0	644 251.0	2.0
$Q(2)B_2^-$	643 415.8	643 423.9	− 8.1
$Q(2)A_2^+$	644 133.3	644 123.5	9.8
$R(1)A_2^+$	668 437.5	668 425.3	12.2
$R(1)B_2^-$	668 681.7	668 661.2	20.5
$R(2)B_2^-$	680 351.9	680 359.3	− 7.4
$R(2)A_2^+$	681 070.0	681 059.0	11.0
$R(3)A_2^+$	692 100.3	692 120.3	− 20.0

Downloaded 08 Mar 2006 to 131.215.225.174. Redistribution subject to AIP license or copyright, see http://jcp.aip.org/jcp/copyright.jsp

TABLE I. (continued).

Transition	Upper band $K=1$ lower $\rightarrow K=2$ lower		
	Observed frequency	Calculated frequency	Obs.-calc.
$R(3)B_2^-$	693 494.4	693 495.1	− 0.7
$R(4)B_2^-$	703 712.5	703 728.2	− 15.7
$R(4)A_2^+$	705 953.9	705 965.2	− 11.3
$R(5)A_2^+$	715 212.8	715 210.0	2.8
$R(5)B_2^-$	718 448.9	718 463.6	− 14.7
$R(6)B_2^-$	726 612.7	726 599.4	13.3
$R(6)A_2^+$	730 972.8	730 983.2	− 10.4
$R(7)A_2^+$	737 936.0	737 936.8	− 0.8
$R(7)B_2^-$	743 526.1	743 515.7	10.4
$K=1$ lower			
$J=1A_2^+ \rightarrow J=2A_2^+$	24 300.784	24 301.7	− 0.9
$J=1B_2^- \rightarrow J=2B_2^-$	25 263.115	25 237.3	25.8
$J=2B_2^- \rightarrow J=3B_2^-$	36 097.344	36 108.3	− 11.0
$J=2A_2^+ \rightarrow J=3A_2^+$	38 209.060	38 182.8	26.3

and assumed that the $E^{\pm}$ state population had thermally relaxed. Our planar supersonic jet expansion is nearly as cold, yielding a jet temperature of 3 K for ArHCl.[13] Under warmer conditions, the E states are observable, as reported by Dyke and co-workers,[2–4] who have measured E state transitions up to $K=4$.

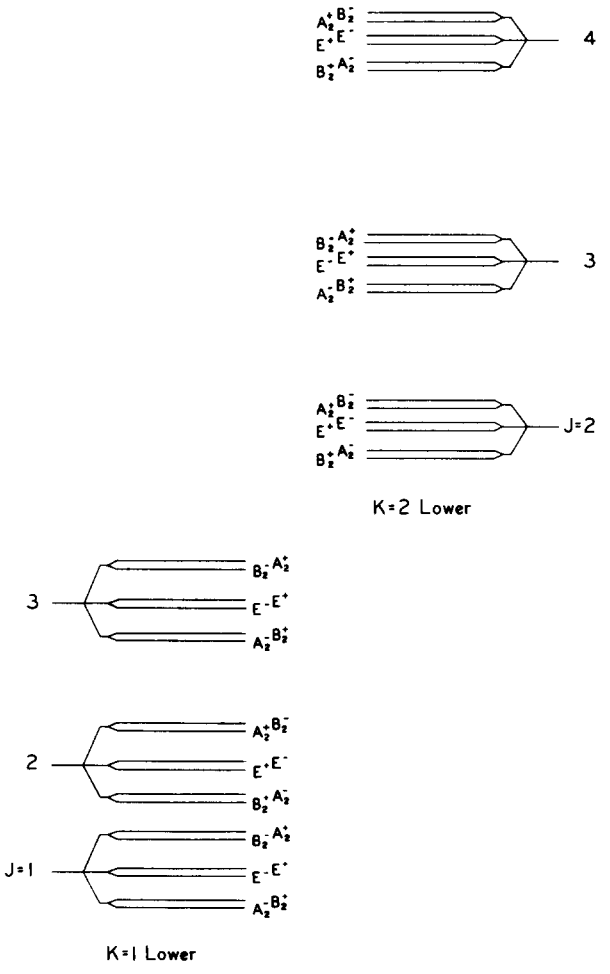

FIG. 5. The energy level diagram for the $K=1$ lower and $K=2$ lower states. For $(H_2O)_2$, the nuclear spin statistical weights are three for A_2 and E states and six for B_2 states.

The 56 rotation–tunneling transitions assigned in this work are listed in Table I and a detailed energy level diagram is shown in Fig. 5. We were able to assign the lowest J states from combination differences calculated from measured transitions in $K=1$ lower from the work of Coudert *et al.*[8] A large number of lines were measured, with essentially no recognizable pattern, and without these combination differences the assignment would have been very difficult. Coudert and Hougen[16] have recently developed a model in which they can include both pure rotational transitions and tunneling–rotational transitions in a combined fit. They included our initial assignments in their fit, along with the microwave data, and they provided us with predictions for higher J transitions. We were subsequently able to either assign new lines from the large number of unassigned spectra, or we went back and searched for new predicted lines. In this way, transitions were eventually assigned as high as $Q(8)$ and $R(8)$. However, the intensity of the P branch was significantly lower and we were not able to measure transitions to as high in J. The assignment of $K=1$ lower as the initial state of these transitions was confirmed by microwave combination differences, which matched to within 2 MHz. For the upper state assignment, there were no combination differences available, and we were not able to determine independently whether it was actually $K=2$ lower or upper. Based only on the fit of Coudert and Hougen, we assign the upper state as $K=2$ lower. Determination of the sign of the asymmetry doubling in $K=2$ lower was unambiguous, given the ordering of the $K=1$ lower states.

The model used here in fitting the present data set is rather simplistic. Because Coudert and Hougen have now developed a much more sophisticated model, it does not seem worthwhile to expend a great deal of effort in improving our model. As discussed previously, in $K=1$ lower, there are three pairs of levels for each J. One pair is made up of the two E states, which were not observed in these experiments. Therefore, two pairs of K-type doublets are observed for each J, split by the geared donor–acceptor tunneling mo-

Downloaded 08 Mar 2006 to 131.215.225.174. Redistribution subject to AIP license or copyright, see http://jcp.aip.org/jcp/copyright.jsp

TABLE II. Fits in which the lower and upper bands are fit independently as two asymmetric vibration–rotation bands. Those constants not listed were set to zero in the fit. Uncertainties are 1σ.

Lower band	Upper band
$(B'' + C'')/2 = 6192.2(4)$ MHz	$(B'' + C'')/2 = 6194.3(10)$ MHz
$(B'' - C'') = 218.8(4)$ MHz	$(B'' - C'') = 238.7(10)$ MHz
$D_J'' = 0.163(7)$ MHz	$D_J'' = 0.133(12)$ MHz
$d_1'' = -0.121(2)$ MHz	$d_1'' = -0.178(7)$ MHz
$(B' + C')/2 = 6155.5(6)$ MHz	$(B' + C')/2 = 6155.3(11)$ MHz
$D_J' = 0.052(5)$ MHz	$\nu = 62\,437.5(69)$ MHz
$\nu = 89\,731.6(26)$ MHz	A(fixed) = 200 000 MHz
A(fixed) = 200 000 MHz	
Standard deviation = 5.9 MHz	Standard deviation = 17.4 MHz

tion. In the present analysis, the transitions originating from the lower pairs of K-type doublets are treated as a vibration–rotation band, and the transitions from the upper pairs of K-type doublets are treated as a second such band. In Table I, lines originating from the lower pairs of states are designated the lower band, and those originating from the upper pairs are designated the upper band. Each band is then fit to a Watson S-reduced Hamiltonian. The vibration in this case, is actually the difference of the acceptor tunneling splittings in $K = 1$ and 2. The approximate frequency for these two bands is then

$$3A + 1/2\nu_{\text{tun}}(K = 1) - 1/2\nu_{\text{tun}}(K = 2),$$

where, in this fit, the sum of the second two terms is the effective vibrational frequency. This is not to imply that the value of A is uniquely determined, however, we assume that it has the proposed value of 6 cm^{-1}. The only quantity actually determined is the sum of the three terms, which is approximately 22 cm^{-1}.

The two vibrational bands were fit separately and the results are shown in Table II. The higher frequency band centered at 670 GHz consisted of the transitions from the lower pairs of states in $K = 1$ lower (A_2^-/B_2^+ symmetry) to the upper pairs of levels in $K = 2$ lower (A_2^+/B_2^- symmetry). Figure 6 contains a plot of the lines observed in this band as well as a characteristic spectrum of one of the transitions. The lower frequency band centered at 644 GHz consisted of the transitions from the upper pairs in $K = 1$ lower (A_2^+/B_2^-) to the lower pairs in $K = 2$ lower (A_2^-/B_2^+). Figure 7 contains a plot of the lines observed as well as a characteristic spectrum of one of the transitions. Also included in the fits of these two bands are several combination differences calculated from the microwave measurements of Coudert *et al.*[8] The difference in frequency between the two bands is the sum of the donor-acceptor tunneling splittings for $K = 1$ lower and $K = 2$ lower, approximately 26 GHz. For the $J = 1$ state of $K = 1$ lower, this splitting has been measured to be 16 GHz; therefore, for $K = 2$ lower it is 10 GHz. The corresponding measured splitting for $K = 0$ lower is 19 GHz.[10]

Fitting these transitions as two vibrational bands is a very simplistic approach and does not explicitly account for

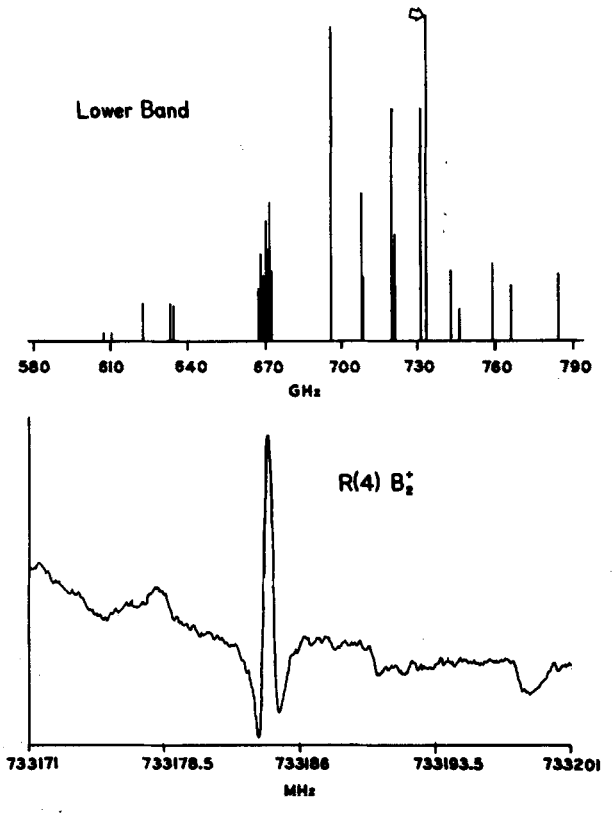

FIG. 6. The upper plot is a stick spectrum of the 670 GHz band for $K = 1$ lower $\rightarrow K = 2$ lower, with the observed intensities. Below is shown a scan of the $R(4)$ B_2^+ transition, marked with an arrow in the stick spectrum.

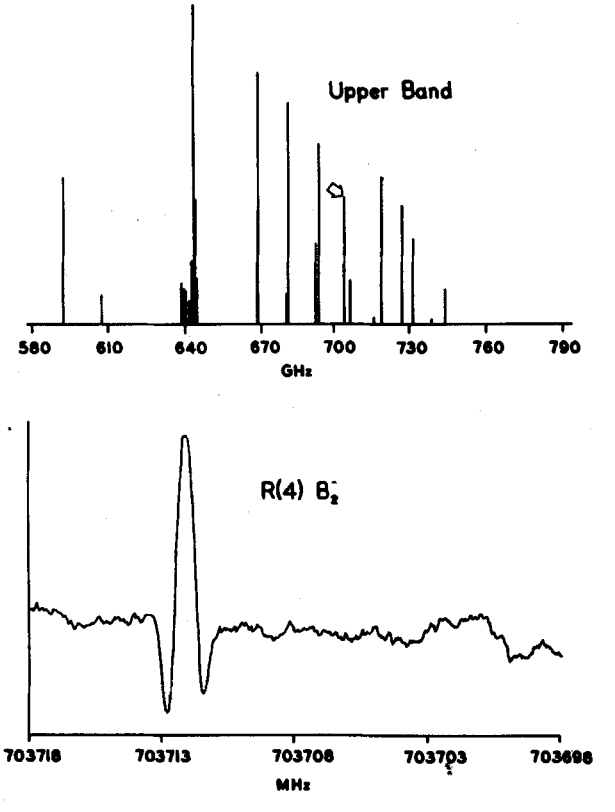

FIG. 7. The upper plot is the stick spectrum for the 644 GHz band of the $K = 1$ lower $\rightarrow K = 2$ lower, with the observed intensities. Below is shown a scan of the $R(4)B_2^-$ transition, marked with an arrow in the stick spectrum.

Downloaded 08 Mar 2006 to 131.215.225.174. Redistribution subject to AIP license or copyright, see http://jcp.aip.org/jcp/copyright.jsp

TABLE III. Fit in which all transitions are fit as a single band including the geared donor–acceptor tunneling splitting. Those constants not listed were set to zero in the fit. Uncertainties are 1σ.

$(B'' + C'')/2 = 6190.2(17)$ MHz
$(B'' - C'') = 228.3(17)$ MHz
$\nu''_{1,5} = 16\,225(13)$ MHz
$D''_J = 0.092(15)$ MHz
$d''_1 = -0.152(9)$ MHz
$(B' + C')/2 = 6153.7(17)$ MHz
$\nu'_{1,5} = 11\,083(17)$ MHz
$\nu = 76\,072(13)$ MHz
A(fixed) = 200 000 MHz
Standard deviation = 40.9 MHz

the J dependence of the geared donor-acceptor tunneling splitting or the correlation between the rotational constants in the various states. As would be expected, the fit is good for low J (up to approximately $J = 4$), with a few MHz standard deviation, but at higher J it deteriorates rapidly. This implies that even for the low J fit, the centrifugal distortion constants are of limited value because they are most likely shifted by the J dependence of the tunneling splitting. It is interesting to note that the higher frequency band, that originating from the lower pair of states, fits much better. A fit was obtained for this entire band with a standard deviation of less than 6 MHz, where for the lower frequency band, the best fit obtained was worse by a factor of three.

A second fit was attempted in which all of the data were fit in a single band, by including a tunneling term in the energy expressions for the upper and lower states. This tunneling term then represents the effective geared donor-acceptor tunneling splitting. Those transitions assigned to the lower band are given a tunneling quantum number equal to -1 and those in the upper band are $+1$. In this fit, an attempt was made to also fit the J dependence of this tunneling; however, it could not be determined. Only a constant tunneling term was determined for $K = 1$ lower and $K = 2$ lower. The results of this fit are shown in Table III. The large standard deviation of the fit (40 MHz) indicates that this is still a grossly oversimplified model for the energy level spacings of the water dimer. However, the analysis is carried out in terms of a single band fit, unlike the first method and a value for the donor–acceptor tunneling splitting is determined for each K state.

One important observation that may be deduced from the results of the fits is that the use of the high barrier approximation in the model of Hougen and Coudert is supported, at least for the states included in the present data set. A comparison of the rotational constants for the lower and upper bands in each K indicates that they are identical within the quoted statistical uncertainties, as expected in the high barrier limit.

There are several possibilities for future work on this project. The first of which would be to measure other rotation-tunneling bands. However, the only allowed transition expected to be sufficiently populated in a supersonic jet is the $K = 0$ lower $\rightarrow K = 1$ upper band. This band is predicted to be at approximately 12 cm^{-1}. In that band, unlike that studied in this paper, the E state transitions, as well as the A_1 transitions, would be observed, which would improve the model and result in a better understanding of the relative contribution of the various tunneling motions to the overall energy level structure. An alternative direction in the study of water dimer is to search for an intermolecular vibrational band. The lowest predicted vibration is the torsion about the acceptor molecule C_2 axis. The lowest energy prediction for this vibration is approximately 80 cm^{-1}, others are as high as 130 cm^{-1}.[17] A third logical step is to attempt to study larger clusters such as the water trimer. We presently have over two hundred lines that are unassigned, many of which are in regions where one would not expect to find dimer transitions, if our understanding of that system is correct. It is very possible that these lines may be due to the trimers, $Ar_2(H_2O)$, $Ar(H_2O)_2$ or $(H_2O)_3$. The water trimer itself is a very complicated system about which very little is known. It has been deduced from deflection experiments[1] that it is only slightly polar and therefore most likely cyclic, having three hydrogen bonds. There is no assigned high resolution spectroscopic data available. Some work has been done on the permutation-inversion theory for water trimer.[18] Our current understanding of water dimer and similar clusters should prove very helpful in assigning the trimer spectrum.

ACKNOWLEDGMENTS

This work was supported by the Director, Office of Energy Research, Office of Basic Energy Sciences, Chemical Sciences Division of the U.S. Department of Energy under Contract No. DE-AC03-76SF00098. The FIR laser system was funded by the National Science Foundation (Grant No. CHE-8612296). We thank Dr. J. T. Hougen and Dr. L. H. Coudert for their interest and guidance in this project.

[1] T. R. Dyke and J. S. Muenter, J. Chem. Phys. **57**, 5011 (1972).
[2] T. R. Dyke and J. S. Muenter, J. Chem. Phys. **60**, 2929 (1974).
[3] T. R. Dyke, J. Chem. Phys. **66**, 492 (1977).
[4] T. R. Dyke, K. M. Mack, and J. S. Muenter, J. Chem. Phys. **66**, 498 (1977).
[5] J. A. Odutola and T. R. Dyke, J. Chem. Phys. **72**, 5062 (1980).
[6] L. A. Curtiss and J. A. Pople, J. Mol. Spectrosc. **55**, 1 (1975).
[7] L. H. Coudert and J. T. Hougen, J. Mol. Spectrosc. **130**, 86 (1988).
[8] L. H. Coudert, F. J. Lovas, R. D. Suenram, and J. T. Hougen, J. Chem. Phys. **87**, 6290 (1987).
[9] Z. S. Huang and R. E. Miller, J. Chem. Phys. **88**, 8008 (1988).
[10] J. A. Odutola, T. A. Hu, D. Prinslow, S. E. O'dell, and T. R. Dyke, J. Chem. Phys. **88**, 5352 (1988).
[11] R. C. Cohen, K. L. Busarow, K. B. Laughlin, G. A. Blake, M. Havenith, Y. T. Lee, and R. J. Saykally, J. Chem. Phys. **89**, 4494 (1988).
[12] K. L. Busarow, G. A. Blake, K. B. Laughlin, R. C. Cohen, Y. T. Lee, and R. J. Saykally, J. Chem. Phys. **89**, 1268 (1988).
[13] K. B. Laughlin, G. A. Blake, R. C. Cohen, D. C. Hovde, and R. J. Saykally, Phil. Trans. R. Soc. London Ser. A **324**, 97 (1987).
[14] J. Farhoomand, G. A. Blake, M. A. Frerking, and H. M. Pickett, J. Appl. Phys. **57**, 1763 (1985).
[15] T. R. Dyke, B. J. Howard, and W. Klemperer, J. Chem. Phys. **56**, 2442 (1972); J. T. Hougen and N. Ohashi, J. Mol. Spectrosc. **109**, 134 (1985).
[16] Coudert and Hougen fit (to be published).
[17] M. J. Frisch, J. A. Pople, and J. E. Del Bene, J. Phys. Chem. **89**, 3664 (1985); R. D. Amos, Chem. Phys. **104**, 145 (1986).
[18] K. Balasubramanian and T. R. Dyke, J. Phys. Chem. **88**, 4688 (1984).

Downloaded 08 Mar 2006 to 131.215.225.174. Redistribution subject to AIP license or copyright, see http://jcp.aip.org/jcp/copyright.jsp